



POLYTECHNIC UNIVERSITY OF BUCHAREST

DOCTORAL SCHOOL: APPLIED CHEMISTRY AND MATERIALS SCIENCE

DOCTORAL THESIS

Functionalized nanoparticle systems for cancer therapy

Author: Ing. Rebecca Alexandra Puiu

Coordinator: Prof. Dr. Ing. Ecaterina Andronescu

2023

Abstract:

Cancer is a disease which origins couldn't be identified, and despite this, it represents the second most deadly disease around the world, heart attacks occupying the first place. At the moment, the only solution to deliver drugs with anti-cancer properties is chemotherapy, but the disadvantage is that it is associated with harmful systemic toxicity, neurotoxicity, gastric conditions, anemia, etc. and also the expected therapeutic result is not achieved due to low solubility and ineffective targeting. These deficiencies of chemotherapy can be avoided or reduced by finding new encapsulation methods for drugs which can offer a better target delivery due to their higher conductivity and stability, and surface morphology.

Despite intensive utilization of chemical drugs like cytostatic, natural therapy gained a lot of interest lately, including essential oils. Researchers who performed *in vitro* and *in vivo* studies so far showed cytotoxic effect against different types of cancer, through apoptosis.

The main purpose of this study is to obtain novel anti-cancer therapies, using both chemical and natural compounds, and different types of delivery systems based on metallic nanoparticles, the efficiency of new systems being analyzed *in vitro*.

Keywords: Nanoparticles, metallic nanoparticles, biotechnologies, cancer treatment, cancer therapy, *in vitro* studies

Table of content

CHAPTER I

I.1. Introduction.....	5
I.2. Nanoparticles – synthesis methods, characterization and usage in biomedical applications	8
I.3. Types of cytostatic for cancer therapy	16
I.3.1. Silver nanoparticles functionalized with cytostatic	19
I.3.2. The usage of essential oils in cancer treatment.....	20
I.3.3. Smart Nanocarriers functionalized with essential oils.....	26
I.4. Use of Silver nanoparticles in cancer therapy.....	29
I.5. Use of SPIONs in cancer therapy.....	31

CHAPTER II

Original contributions and general conclusions

II.1. Choice of theme justification.....	33
II.2. MAPLE Technique	33
II.3. Biological studies of silver nanoparticles functionalized with cytostatic.....	35
II.4 General conclusions.....	38

CHAPTER III

Bibliography.....	41
Publications.....	54

1. Introduction

Cancer represents the biggest problem in medicine worldwide, scientists looking permanently for a sustainable treatment and a complete cure for the oncology area. The main objective of finding different approaches to prevent its progression is achieving personalized therapy by targeting molecular pathways. This field is very dynamic, every discovery of drugs and therapies leading to a new perspective about cancer progression [1]. Even if recently special attention has been paid to studies focused on cancer treatment, chemotherapy, together with radiotherapy and surgery still represent the standard of care for oncologic patients [2].

Tissues invaded by tumors are known to have high vascular density, their growth being maintained by blood supply. A vascular architecture which is defective, combined with a low lymphatic drainage, leads to EPR effect (enhanced permeation and retention) [3]. New therapeutic approaches are really required to deliver therapeutic agents to location of tumor in a specific way and a rapid answer to this situation is nanotechnology' development, using nanomaterials in cancer therapy[4] .

Depending on the desired physiological response, nanocarrier systems can be tailored in well-controlled ways, to interact with target tissue, having different forms: micelles, dendrimeres, nanoparticles, nanofibers, nanotubes, quantum dots, etc. There are two main reasons why cancer appears: a decrease in cell death, or increased cell proliferation. Through different extern actions, cell death can be programmed, without affecting healthy cells [5]. One example is targeted therapy, which is different from chemotherapy in terms of personalized therapy. In this case, nanoparticles with suitable size and charge can be used as a carrier, impacting the drug delivery area. Nanoparticles has many advantages, like nonspecific uptake, increased solubility, and low side effects [6].

Nanotechnologies represent a new option in the diagnosis and treatment of cancer, offering unique properties possessed by materials with a nanometric scale that have addressability in various fields of science and medicine. A wide range of nanomaterials has been studied so that they can be used both for diagnostic (bioimaging, nanobiosensors) and therapeutic purposes (nanocarriers, immunotherapy, photodynamic therapy) [7].

Nanomaterials represent an interesting chapter for cancer treatment due to their indisputable properties, one of them being the tunable surface, meaning that a wide variety of

drugs and molecules can be attached to it. Surface-modified nanocarriers presents as a consequence improvement of important issues on long-term, like drug metabolism and decreased solubility.

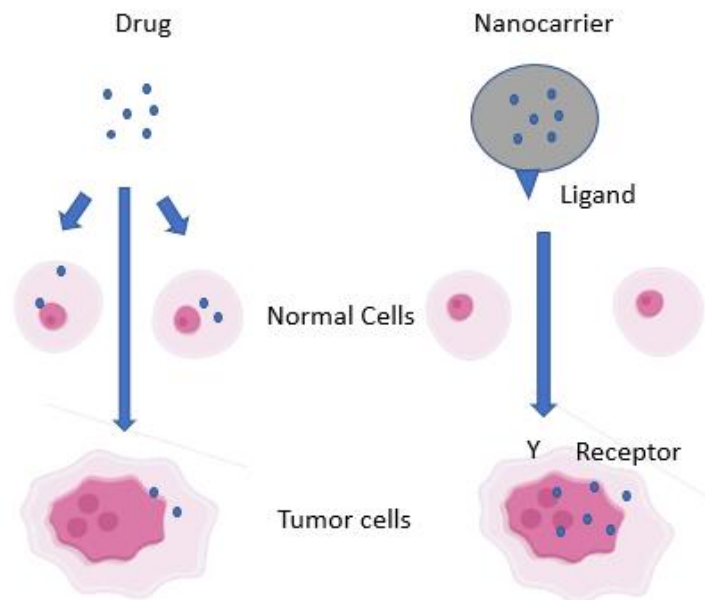


Figure 1. Comparison between targeted and untargeted drug delivery

More than that, nanocarriers can also act as passive target, this being called the EPR effect (enhanced permeation and retention), the deposition of drugs directly into the tumor being increased [8]. Thereby, the penetration of the tumoral tissue and the accumulation of nanoparticles in the tumor are facilitated, in contrast with healthy tissues [7].

I.2. Metal Nanoparticles – synthesis method, characterization and usage in biomedical applications

The interest of using metallic nanoparticles in cancer therapy and biomedicine is increasingly more and has the main challenge of limiting the contact between their surface and the healthy cells to target only the cancerous cells and specific tissues. The current literature presents many studies regarding the production and optimization process of nanoparticles, which are divided into two categories: metallic (Au, Pt, Ag, etc.) and nonmetallic (polylactic-co-glycolic acid, carbon nanotubes, etc) and can be obtained through three different methods; physical, chemical and based on microorganisms (green synthesis) [9].

Cancer therapy is the area of interest in which nanoparticles are constantly used. An important aspect that may change cancer treatment is that cancer cells present resistance to a large variety of lipophilic drugs, causing drug resistance and ineffectiveness of chemotherapy. Various studies reported that metallic nanoparticles with a highly reactive surface can induce apoptosis, which is considered the most effective method to eliminate cancer from organisms, due to their ROS ability [10].

Plenty of studies from recent literature confirms the effects of metallic nanoparticles in anti-cancer therapy: silver nanoparticles shows positive effects on breast cancer cells, gold nanoparticles showed cytotoxicity of 70% on colorectal adenocarcinoma cells, CeO₂ nanoparticles showed effective activity on lung cancer [9].

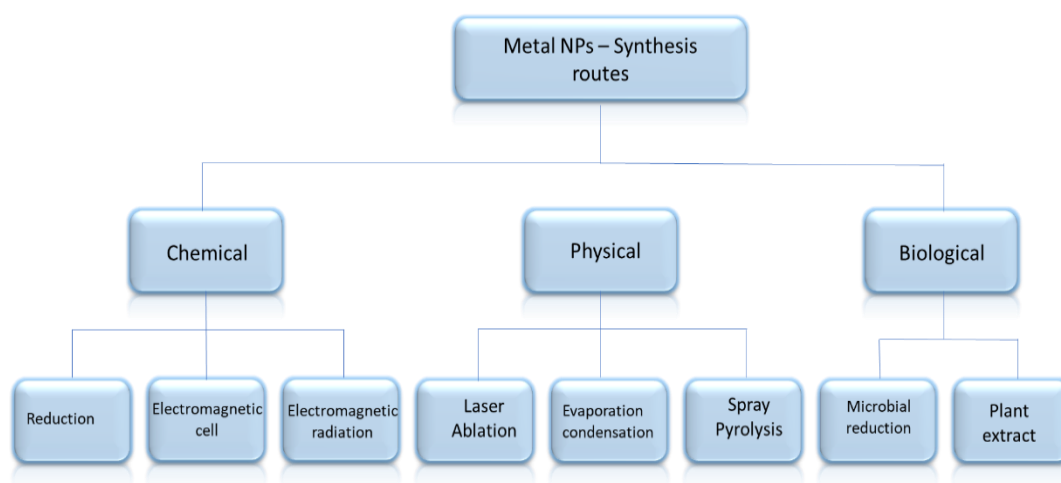


Figure 2. Synthesis methods of Metal nanoparticles

There are plenty of synthesis routes to obtain metal nanoparticles, as it can be seen in figure 2, which require special vacuum conditions, performant instruments and different chemical additives, but there are also some unpleasant factors when using chemical methods, due to increased biological risks to the environment.

Particles with a nanometric size possess both molecular and atomic settings in nanometer range, with different sizes and shapes and improved characteristics of their surface which can be customized. Surface to volume ratio of metal nanoparticles is large, its production becoming interesting at a global level for biomedical field [11]. The main three properties are modified: physical, chemical and biological, including cellular uptake, distribution in the

tumor, mechanical properties, melting point, agglomeration, thermal conductivity, compared with the material in a bulk size [12].

There are many unique properties of metal nanoparticles used in cancer therapy, like morphology, crystallinity, size, surface properties and, last but not least, composition. These properties may be altered during conjugation with various types of drugs, but there are available different techniques which can offer relevant parameters about studied nanomaterials, to describe in detail its physicochemical properties (Table 1).

Table 1: Common techniques used to characterize metal nanoparticles

Category	Technique	Observation	Reference
Spectroscopy	XRD (X-Ray Diffraction)	Crystallite size, composition, crystal structure	[13]
	FT-IR	Composition of chemical surface, crystal structure, nature of bonds	[14]
	UV-VIS	Size, agglomeration, concentration	[15]
	Raman	Molecular interactions, chemical structure	[16]
Electron microscopy	TEM	Morphology (it affects cells interaction), elemental composition of nanoparticles	[17]
	SEM	Morphology (it affects cells interaction), size of nanoparticles	[14]
Surface charge determination	ELS Streaming potential (electrophoretic light scattering)	Stability of nanoparticles, zeta potential, determination of surface charge	[18]
Scattering method	DLS (dynamic light scattering)	Size distribution, agglomeration	[19]
	SAXS (small-angle X-ray scattering)	Size, growth coefficient	[20]

	NTA (nanoparticle tracking analysis)	Size distribution	[21]
Surface analysis	BET	Surface area	[22]

I.3.1. Silver nanoparticles functionalized with cytostatic

Several tests performed in vivo and in vitro throughout the time showed that silver nanoparticles tend to agglomerate within different types of cells, having an affinity for macrophages and reticuloendothelial cells. Similar, they are also accumulating in various tissues as liver, spleen, lymph nodes, kidney, bone marrow. An important role in renal clearance plays nanoparticles' size, this also enhancing circulation time [23].

Using nanoparticles to encapsulate chemotherapeutic drugs to target cancer cells is a new method used to reduce toxicity and side effects associated with cytostatic administration [24]. Considered one of the most used antibacterial agents, silver nanoparticles present a limited resistance upon contact with bacteria, and low toxicity to normal cells. Studies and researchers in nanotechnology domain also showed that silver nanoparticles can be successfully used in medicine, due to their multi-drug-resistance capability, antifungal, antiviral and antibacterial effects [25]. Synthesis route of silver nanoparticles is both environmental friendly and cost effective, making them a promising agent for cancer treatment [26].

In literature, synthesized silver nanoparticles have sizes more than 10nm. Because the parameters of chemical reactions depends on the shape and size of the particles, it is very likely that nanoparticles with smaller sizes to be less toxic for non-cancerous cells and to target the cancer cells directly [27].

One of the most efficient chemotherapeutic drug from taxane family is Paclitaxel, showing anti-tumoral activity against a many late-stage types of cancer, including ovarian, breast or lung cancer, advanced prostatic cancer, having a big potential of triggering apoptosis [28]. The anticancer effect is promoted by causing cell death due to microtubules stabilization and inhibiting cell cycle phases [29]. Paclitaxel has a low therapeutic index, are not very soluble in water and due to its low permeability, it can cause a wide variety of side effects [27].

Silver nanoparticles can be successfully combined with various anti-cancer drugs, one of them being Paclitaxel. Kalındemirtas et al. found a potent cytotoxic effect of AgNPs-PTX on osteosarcoma cell line (Saos-2), a fatal and very rare type of cancer, appearing more often to young adults and adolescents. Silver nanoparticles act as carrier, solving solubility and toxicity problems caused by Paclitaxel. The study also showed that the dosage of the drug known to have serious side effects can be reduced 10 times and also cytotoxicity on normal cells is missing, indicating that the drug carried out by silver nanoparticles target specifically the cancer cells [27].

In-vitro studies demonstrated that size of silver nanoparticles is a very important factor related to their performance – it increases as the size decreases. This experiment also showed a higher therapeutic efficacy, without appearance of systemic toxicity [30].

I.3.2. The usage of essential oils in cancer treatment

Even if cytostatic drugs, as the one tested in the current thesis: fludarabine, paclitaxel, doxorubicin, gemcitabine and carboplatin offer an substantial clinical response during anti-cancer treatment, there are still some issues for which there are limited solutions: drug resistance, cancer recurrence, healthy tissues being damaged by lack of selectivity [31].

Phytochemicals, which are natural substances with an increased biological activity, can be another solution for cancer treatment, inducing apoptosis. Essential oils extracted from aromatic plants, have antiproliferative, antioxidant, and antimutagenic properties and can be an adjuvant to help increase the sensitivity of tumor cells, being a viable alternative to conventional treatment [31].

There are more than 300 types of essential oils used in different domains, mostly of them being liquids at room temperature. Essential oils can be soluble both in ether and alcohol, but insoluble in water, volatile in nature, and instable when are in contact with light, oxygen and heat [12].

All essential oils are volatile, have a density less than 1 and possess a low molecular weight, but their biological properties differs depending on their structure and chemical constitution [32].

I.5. Use of SPIONs in cancer therapy

There are a lot of systems of nanocarriers available, like organic and inorganic polymers, metal oxides, lipids, etc., but lately, an increased attention was gained by superparamagnetic iron oxide nanoparticles, also known as SPIONs, due to remarkable properties of magnetic guidance [33]. Among all properties of SPIONs, most remarkable are magnetic sensitivity [34], biocompatibility and that can also be used for targeting the tumor and drug delivery simultaneously [35]. Having an enhanced permeability, SPIONs can target tumoral zones and are FDA approved to be used in clinical applications [36]. After administration, temperature of targeted area increases, and death of tumoral cells is induced.

Another reason why SPIONs are used in biomedical application, are low toxicity, no remnant magnetization [37]. Despite all of these characteristics, magnetite tend to decrease surface energy and therefore, SPIONs should be modified with other biocompatible materials in order to avoid agglomeration [35]. These obstacles occur *in vivo*, major challenges happening due to decreased colloidal stability and circulation time through the blood [38].

A complex used for cancer therapy are SPIONs loaded with cyclodextrins (a glucose compound), an useful candidate for hydrophobic drugs due to their exterior which is hydrophilic and the hydrophobic interior [39]. There is a study in which a drug delivery system with high stability was formed by interaction of SPIONs with β -cyclodextrin and paclitaxel, to improve magnetic guidance. The developed complex showed antitumoral activity both *in vitro* and *in vivo* analyses [40].

There are plenty of studies performed on iron oxide nanoparticles, showing their efficacy in cancer therapy. Krus et al. studied production of ROS by iron nanoparticles, which helped increasing cytotoxic effect [41]. In another study, iron oxide nanoparticles enhanced cell death by apoptosis. This approach can be dangerous because nanoparticles can not be fully cleared from the body, that's why it should be taken care that the size of nanoparticles to be as small as possible [30].

Nanoparticles which have an iron oxide core leads to avoid unwanted effects by directing nanoparticles into the tumor using external magnets. These kind of nanoparticles are also called superparamagnetic nanoparticles, possessing anisotropy contributions to improve standard therapies [42].

2. Objectives and choice of theme justification

Lately, studies reported that cancer incidence is more and more seen in young patients, with ages between 20 and 29 years old. Cancer incidence is lower with 30% in men, and in case of women with ages between 30 and 39 years, cancer prevalence is almost twice [43]. Unfortunately, young females who survive to cancer treatment, become more vulnerable to its adverse reactions, having cardiovascular diseases or infertility. Also, regarding this subject, studies shows that women survivors become 38% less fertile after chemotherapy than others, main driver being ovarian injury [44].

Chemotherapy represent the most convenient method to be used for all forms of cancer, and is based on dose intensity, meaning that a maximum tolerated dose should be established every month. This method may divide cancer cells, but unfortunately may also affect normal cells division, causing a variety of adverse reactions after chemotherapeutic treatment. It is important to administer cytostatic at an established time interval, allowing in this way normal cells recovering – process which may go to cancer cells resistance. Thus, there is a huge need of new strategies and therapies to avoid side effects of chemotherapy, combating the disadvantages [45].

II.2. MAPLE Technique

MAPLE Technique is also known as Matrix-assisted pulsed laser evaporation, and is a more delicate laser method, designed for very thin biomolecular films, keeping their original structure and functions. In comparison with other methods of laser deposition, MAPLE offer some excellent advantages [46]:

- The obtained coatings are homogenous, even the composites
- The deposited materials are versatile
- The depth and adherence of coatings can be controlled over any kind of substrate

In addition to all the advantages presented so far, the main one offered by combination of matrix with wavelength and fluence is the ability to keep the properties (physicochemical and chemical) of the organic molecule.

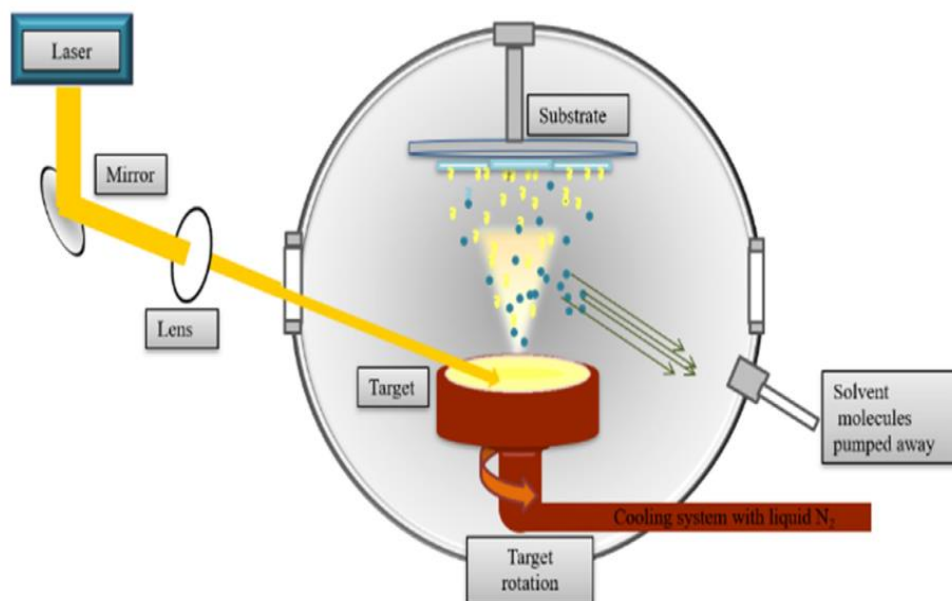


Figure 3 MAPLE installation [46]

In Fig. 3 can be seen a typical MAPLE installation, consisting in a pulsed laser which can be infrared or ultraviolet, a beam spot with a range between 1-25mm² which passes through a vacuum chamber on a solid target. The laser fluence is chosen to avoid target' degradation, and is included between 0.100J/cm² and 5 J/cm².

The target include a matrix frozen with liquid nitrogen, which contains organic molecules dissolved in absorbent solvent. The homogeneity of the target is vital, the concentration being kept so that the studied material can be fully dissolved until it can form a homogeneous solution. Adhesion coefficient of volatile molecules is very low and they can be eliminated by the vacuum system, so the solvent molecules forms a coating after being collected on a substrate. Because a low concentration is being used, we can find out that the molecules from target material are protected by high volatile molecules of solvent matrix, avoiding thermal damage during laser interaction [47].

3. Original contribution

Anti-Cancer Nanopowders and MAPLE-Fabricated Thin Coatings Based on SPIONs Surface Modified with Paclitaxel Loaded β -Cyclodextrin

In the first study, we developed smart nano-engineered targeted drug-delivery systems with tailored pharmacokinetics and biodistribution which can selectively deliver anti-cancer agents directly to the tumor site are the solution to most difficulties encountered with conventional therapeutic tools. Here, we report on the synthesis, physicochemical characterization, and in vitro evaluation of biocompatibility and anti-tumor activity of novel magnetically targetable SPIONs based on magnetite (Fe_3O_4) nanoparticles' surface modified with β -cyclodextrin (CD) and paclitaxel (PTX)-guest-host inclusion complexes ($\text{Fe}_3\text{O}_4@ \beta\text{CD}/\text{PTX}$).

Fe_3O_4 - β -cyclodextrin nanoparticles ($\text{Fe}_3\text{O}_4@ \beta\text{-CD}$) were prepared by the co-precipitation method, which involves base-induced simultaneous precipitation of ferrous (Fe^{2+}) and ferric (Fe^{3+}) ions in an aqueous solution. In brief, solution 1 (Sn1) was prepared by dissolving ferrous sulfate and ferric chloride (molar ratio 1:2) in 300 mL demineralized water. Solution 2 (Sn2) consisted of 1 g β -CD and 9 mL ammonium hydroxide in 300 mL demineralized water. Next, Sn 1 was added dropwise into Sn2 using a pressure-equalizing dropping funnel under magnetic stirring. The precipitated magnetite nanoparticles were magnetically collected. After decantation of the liquid phase, the resultant powder was thoroughly washed three times with demineralized water and left to air dry at room temperature.

The nanopowders were fully characterized by X-ray powder diffraction (XRD), scanning electron microscopy (SEM), transmission electron microscopy (TEM), Fourier transform infrared spectroscopy (FT-IR), and thermal analysis (simultaneous thermogravimetric analysis (TGA) and dynamic scanning calorimetry (DSC)).

PTX- β -CD inclusion complexes were prepared by the solvent evaporation method. To this end, 100 mg $\text{Fe}_3\text{O}_4@ \beta\text{-CD}$ nanoparticles were redispersed in a solution of PTX (10 mg) in chloroform (1 mL) was added and mixed in a grinding mortar until complete evaporation of chloroform. This was subsequently stored at 5°C for further use.

$\text{Fe}_3\text{O}_4@ \text{PTX}$ -loaded β -CD thin films were obtained by MAPLE technique. These were deposited on glass and Si substrates which previously have been successively cleaned with acetone, ethanol, and deionized water in an ultrasonic bath for 15 min. The substrates were

dried under a high purity nitrogen stream. The MAPLE targets consisted of a 2% suspension of Fe₃O₄@β-CD/PTX inclusion complex nanocomposites in DMSO which was poured into a pre-cooled target holder at 173 K and subsequently immersed in liquid nitrogen for 30 min. The MAPLE depositions were performed using a KrF* excimer ($\lambda = 248$ nm and $\tau_{FWHM} = 25$ ns) COMPexPro 205 model, Lambda Physics-Coherent (Göttingen, Germany), that was operated at a repetition rate of 15 Hz. Three different fluences of the laser beam, i.e., 300, 400, and 500 mJ/cm², respectively, were investigated. A number of laser pulses ranging between 22,000 and 75,000 were applied to each target. During the deposition process, the experimental parameters (i.e., substrate temperature, background pressure, and target to substrate distance) were maintained constant (room temperature, 1 Pa, 4 cm, respectively).

The crystallinity of Fe₃O₄@β-CD nanopowders was investigated by XRD analysis. X-ray diffraction patterns were recorded at room temperature using CuK α radiation ($\lambda = 1.54056\text{\AA}$ at 15 mA and 30 kV) with the Bragg diffraction angle 2θ ranging between 10 and 80°.

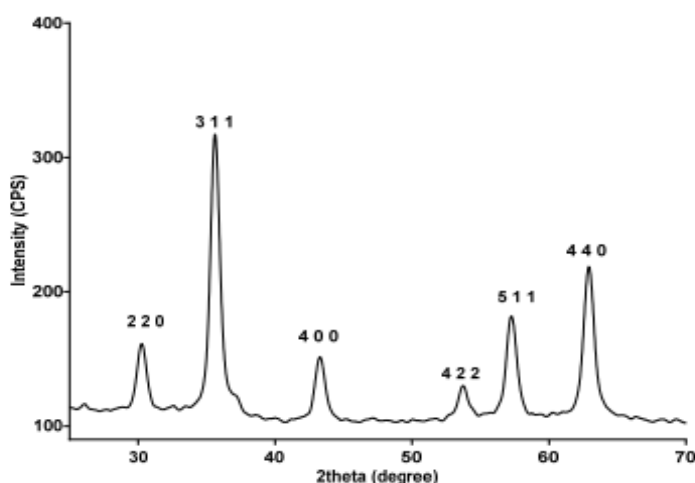


Figure 4. XRD patterns of fabricated Fe₃O₄@ β-CD nanopowders

Sharp diffraction peaks appearing at $2\theta = 30.31, 35.71, 43.31, 53.90, 57.61,$ and 62.81 were assigned to the (2 2 0), (3 1 1), (4 0 0), (4 2 2), (5 1 1), and (440) planes of the magnetite lattice, respectively, being in good agreement with the literature [48].

The inner structure and morphology of the nanocomposites were investigated by TEM. The TEM images of the Fe₃O₄@ β-CD nanopowders are plotted in Figure 5. At higher magnifications, one can distinguish a nanocrystalline magnetite phase without agglomeration and a low-ordered non-crystalline shell that can be attributed to the β-CD coating (Figure 5b).

The recorded SAED ring pattern plotted in Figure 5d corresponds to the (220), (311), (400), (422), and (511) magnetite lattice planes being in perfect agreement with the high polycrystallinity of the magnetite phase and confirming once again the absence of any other crystalline phase.

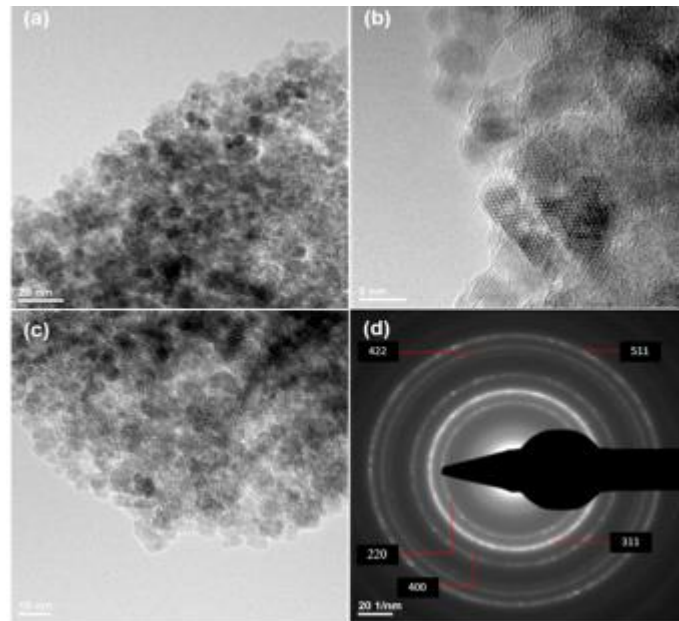


Figure 5. TEM (a,b,c) micrographs and SAED pattern (d) of Fe₃O₄@ β-CD nanopowders.

The shape and size nano-details of the surface of the Fe₃O₄@ β-CD composites were evaluated by SEM analyses performed on an FEI electron microscope, using secondary electron beams with energies of 30 keV.

Agglomerated nanoparticles can be observed in the low-magnification (5000×) SEM micrograph (Figure 6a). High-magnification images (400,000×) revealed 3–5 nm-sized nanoparticles of well-defined spherical morphology (Figure 6 b,c,d). SEM was also used to determine the MAPLE-fabricated thin films' particle size, shape, and morphological and textural features. Figure 7a is an SEM micrograph at 200,000 × magnification of the cross-section of a Fe₃O₄@β-CD nanocomposite thin films deposited at 400 mJ/cm² laser fluence. One can observe the uniform, compact, and agglomerated morphology of the film. The film's surface exhibits an irregular aspect with thicknesses varying from 18 nm up to 71 nm (Figure 7b).

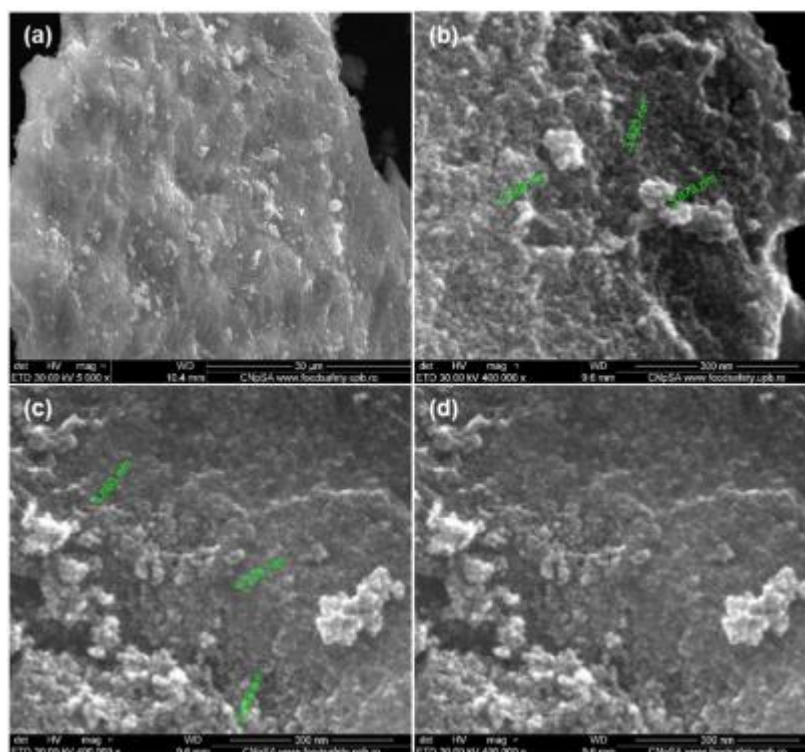


Figure 6: SEM micrographs of Fe₃O₄@β-CD nanopowders at (a) low-magnification (5000×) and (b,c,d) high-magnification (400,000×)

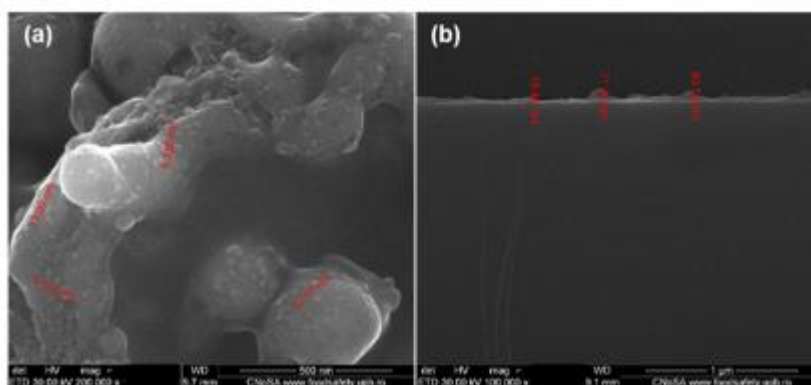


Figure 7: Plain view (a) and cross-section (b) SEM micrographs of Fe₃O₄@β-CD/PTX deposited at 400 mJ/cm²

In order to evaluate the biocompatibility of our novel MAPLE-fabricated magnetic films represented by Fe₃O₄@β-CD nanoparticles, we carried out simple cytotoxicity assays on a normal 3T3 osteoblast cell line culture. No change in cell viability was observed in the presence of the bare β-CD modified magnetite after performing MTT test (Figure 8a), and the level of NO in the culture medium was similar to the control (Figure 8b). The good biocompatibility of this Fe₃O₄@β-CD nanocoating was also confirmed by phase-contrast

microscopy, as no evident adverse effect on the morphology of normal osteoblasts was seen in Figure 9.

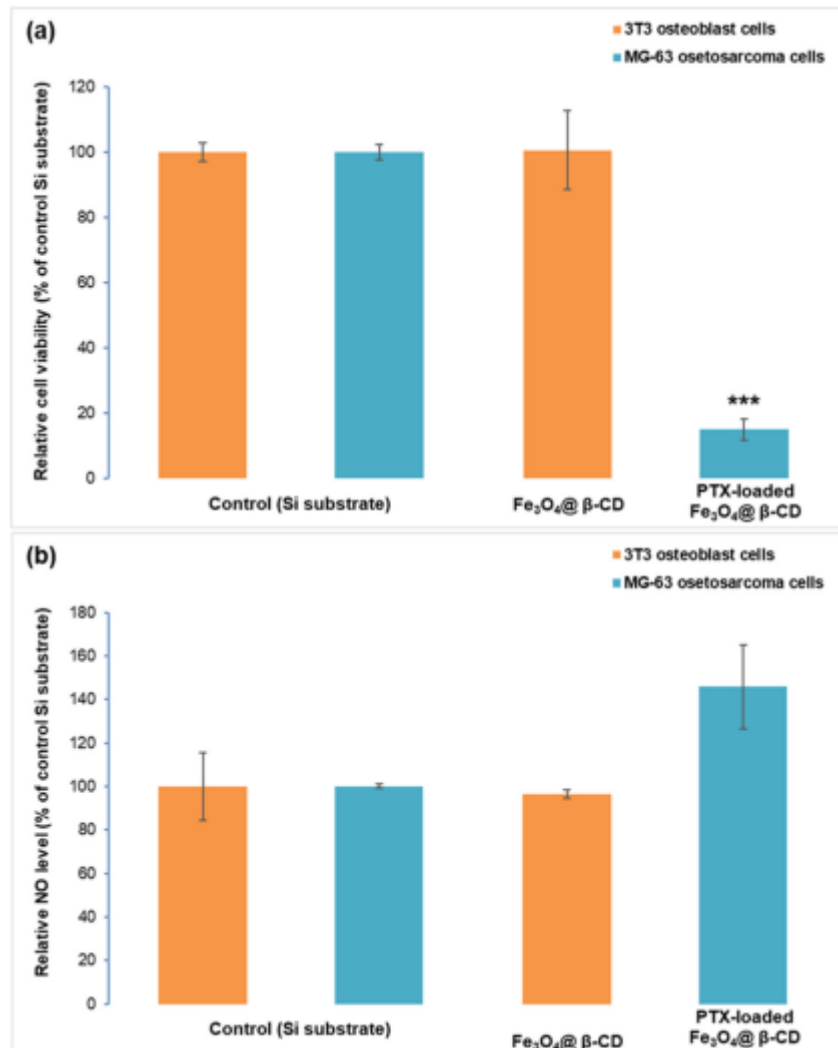


Figure 8. Biocompatibility of Fe₃O₄@β-CD nanoparticles on normal 3T3 osteoblasts (a) and anti-tumor efficiency of PTXloaded Fe₃O₄@β-CD nanocomposites on MG-63 osteosarcoma cells (b) evidenced by the results of MTT (a) and Griess (b) assays. The results were calculated as mean values (n = 3) and expressed relative to control samples (***) p < 0.001).

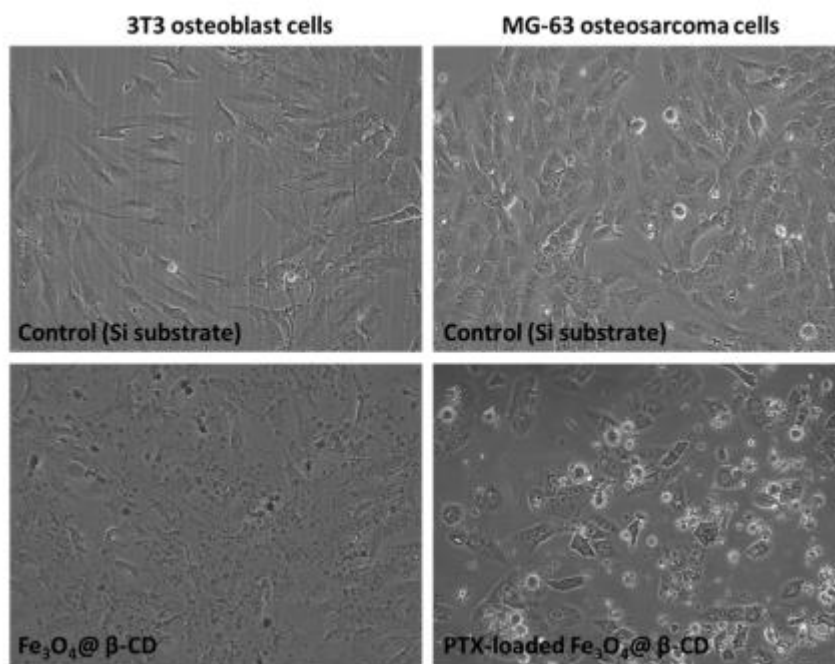


Figure 9. Images of phase-contrast microscopy of normal 3T3 osteoblasts and MG-63 osteosarcoma cells cultured on the surface of Fe₃O₄@β-CD nanocoating and PTX-loaded Fe₃O₄@β-CD nanocomposites, respectively. Objective used: 10×.

A significant decrease to 85% of control (represented by a simple glass slide) proved the high efficiency of PTX-loaded β-CD surface modified SPIONs deposited as thin films by MAPLE technique on glass substrates (Figure 8a). Comparing the poor antitumoral activity of the free drug with the high efficiency of PTX-loaded β-CD surface modified SPIONs deposited as thin films by MAPLE, we concluded that these modified surface have improved activity and great potential for anti-cancer applications. The NO level rose to 145% of the control (Figure 8b), suggesting the inflammatory effect induced by these PTX-loaded nanocomposites. Only a few tumor osteoblasts were noticed after 24 h of incubation with PTX-loaded Fe₃O₄@β-CD nanocomposites in the phase-contrast microscopy images (Figure 9).

The pristine β-CD surface-modified nanopowders and thin films showed excellent biocompatibility and nocyctotoxic effect. On the other hand, magnetic thin films loaded with the anti-cancer drug PTX exhibited significantly increased affinity for tumoral cells.

Multifunctional Polymeric Biodegradable and Biocompatible Coatings Based on Silver Nanoparticles: A Comparative In Vitro Study on Their Cytotoxicity towards Cancer and Normal Cell Lines of Cytostatic Drugs versus Essential-Oil-Loaded Nanoparticles and on Their Antimicrobial and Antibiofilm Activities

Second study performed was a comparative in vitro study of selective cytotoxicity against MCF7 tumor cells and normal VERO cells tested on silver-based nanocoatings synthesized by the matrix-assisted pulsed laser evaporation (MAPLE) technique. Silver nanoparticles (AgNPs) were loaded with five representative cytostatic drugs (i.e., doxorubicin, fludarabine, paclitaxel, gemcitabine, and carboplatin) and with five essential oils (EOs) (i.e., oregano, rosemary, ginger, basil, and thyme). The as-obtained coatings were characterized by X-ray diffraction, thermogravimetry coupled with differential scanning calorimetry, Fourier-transform IR spectroscopy, IR mapping, and scanning electron microscopy.

The aim of the present study was to comparatively assess the cytotoxic activity against MCF7 tumor and healthy VERO cell lines of classic cytostatic/natural-EO-loaded AgNPs embedded in a biodegradable and biocompatible polymeric matrix obtained by MAPLE for anti-tumoral applications. In addition, the antimicrobial and antibiofilm activity of the prepared nanocoatings against representative model bacterial and fungal strains, namely *Staphylococcus aureus* (*S. aureus*), *Escherichia coli* (*E. coli*), and *Candida albicans* (*C. albicans*), was also tested.

While all nanocoatings loaded with antitumor drugs exhibited powerful cytotoxic activity against both the tumor and the normal cells, those embedded with AgNPs loaded with rosemary and thyme EOs showed remarkable and statistically significant selective cytotoxicity against the tested cancer cells. The EO-loaded nanocoatings were tested for antimicrobial and antibiofilm activity against *Staphylococcus aureus*, *Escherichia coli*, and *Candida albicans*. For all studied pathogens, the cell viability, assessed by counting the colony-forming units after 2 and 24 h, was significantly decreased by all EO-based nanocoatings, while the best antibiofilm activity was evidenced by the nanocoatings containing ginger and thyme EOs.

AgNPs were prepared by the bottom-up chemical reduction method. In brief, solution 1 (Sn1) was prepared by dissolving 0.5 g AgNO₃ in 100 mL of distilled water. Solution 2 (Sn2) consisted of 1 g D-glucose and 4 g NaOH dissolved in 400 mL distilled water at the temperature of 80 °C under magnetic stirring. In the next step, Sn1 was added dropwise using a pressure-equalizing dropping funnel into Sn2 under magnetic stirring. In the case of AgNPs

functionalized with cytostatic agents, 100 mg of doxorubicin, fludarabine, carboplatin, gemcitabine, and paclitaxel were added to Sn2, and in the case of AgNPs functionalized with EOs, 200 μ L of rosemary, basil, thyme, oregano, and ginger were added to Sn2. At this step, the obtained precipitate was collected, and after decantation of the liquid phase, the resulting powder was washed three times with demineralized water and dried at room temperature (RT).

Table 2 introduces the sample codes of all the materials used in this study.

Table 2: Sample codes of all the materials utilized and their description

Sample Code	Description	Sample Code	Description
AgNPs@doc	silver nanoparticles functionalized with doxorubicin	AgNPs@ros	silver nanoparticles functionalized with rosemary
ANPs@car	silver nanoparticles functionalized with carboplatin	AgNPs@bas	silver nanoparticles functionalized with basil
AgNPs@flu	silver nanoparticles functionalized with fludarabine	AgNPs@thy	silver nanoparticles functionalized with thyme
AgNPs@gem	silver nanoparticles functionalized with gemcitabine	AgNPs@ore	silver nanoparticles functionalized with oregano
AgNPs@pac	silver nanoparticles functionalized with paclitaxel	AgNPs@gin	silver nanoparticles functionalized with ginger

The XRD patterns of the AgNPs can be observed in Figure 10. Four diffracted intensities in the range 20° – 80° were measured. The XRD patterns confirm the cubic crystal structure of the AgNPs. Specific peaks were identified at 2θ values of 38.45° , 46.35° , 64.75° , and 78.05° , which correspond to the (1 1 1), (2 0 0), (2 2 0), and (3 1 1) diffraction plans of the AgNP crystals.

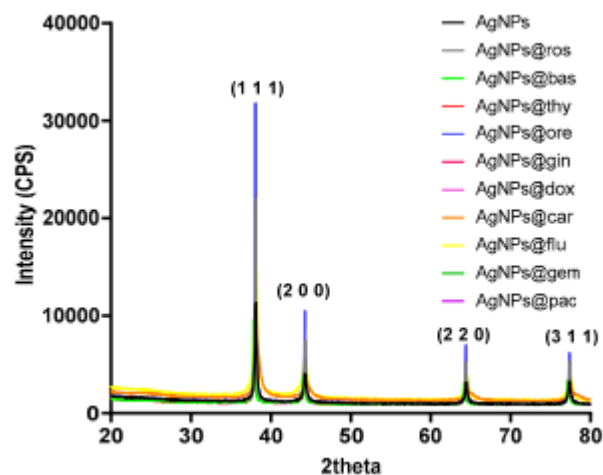


Figure 10: XRD patterns of AgNP powders

The SEM micrographs (Figure 11) show the nanometric size of the AgNPs. The particles have a quasi-spherical shape, with diameters varying from 20 to 60 nm. In addition, it can be observed that the AgNPs functionalized with EOs have higher diameters than those functionalized with cytostatic drugs. Most likely, this phenomenon is due to the complexity of the EOs that contain hundreds of compounds, while cytostatic drugs are composed of single molecules.

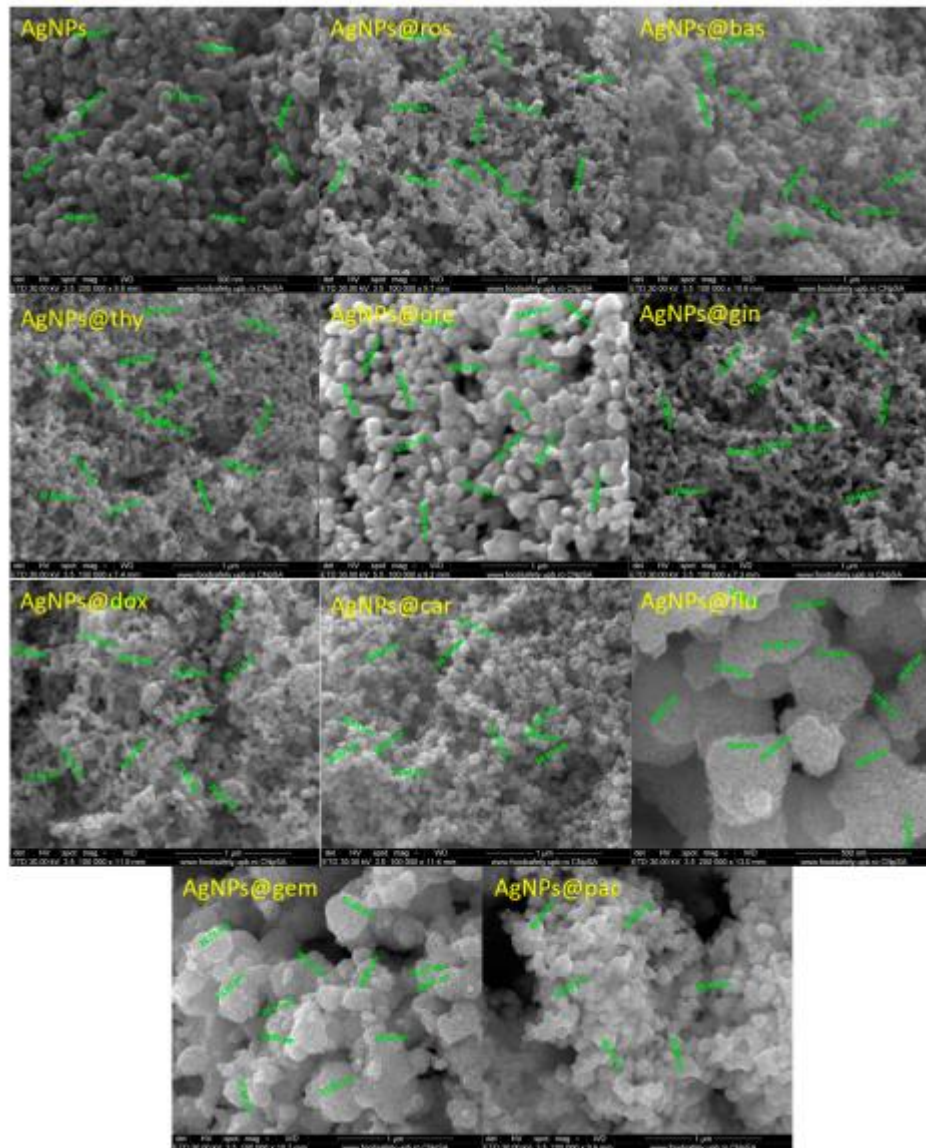


Figure 11: AgNPs functionalized with different cytostatic drugs and essential oils

Figure 12 presents micrographs of surface nanocoatings fabricated at laser fluences ranging from 200 to 600 mJ/cm² (Figure 12a–e). According to Figure 12, the surfaces are wellcovered with PHBV/AgNPs. In all samples, the surfaces present agglomerates consisting of embedded materials well dispersed in the polymer matrix. An increased uniformity of the

surface could be observed in the case of the nanocoatings obtained at a laser fluence of 400 mJ/cm² (figure 12c).

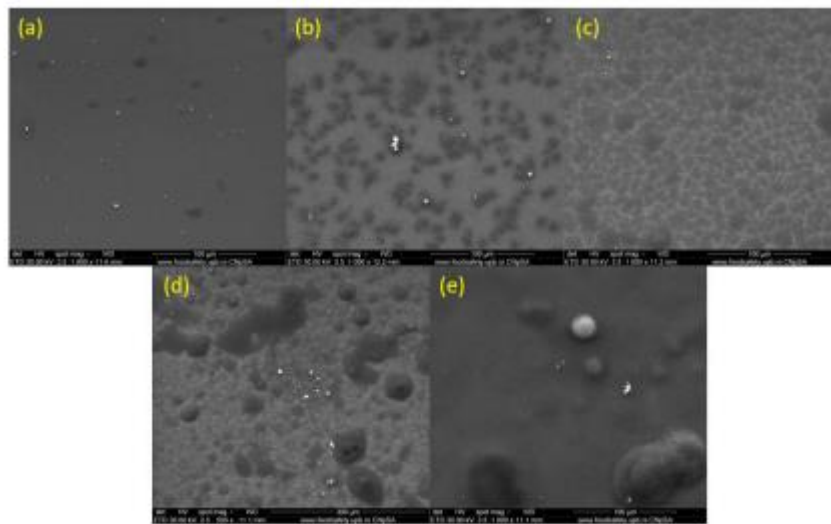


Figure 12: SEM images of PHBV/AgNPs coatings at 1000× (a–e), obtained at laser fluences of (a) 200 mJ/cm²; (b) 300 mJ/cm²; (c) 400 mJ/cm²; (d) 500 mJ/cm²; and (e) 600 mJ/cm².

The morphological characteristics of all composite coatings can be observed in Figure 13. The coatings had a uniform deposition, and some agglomerates were present on the surface.

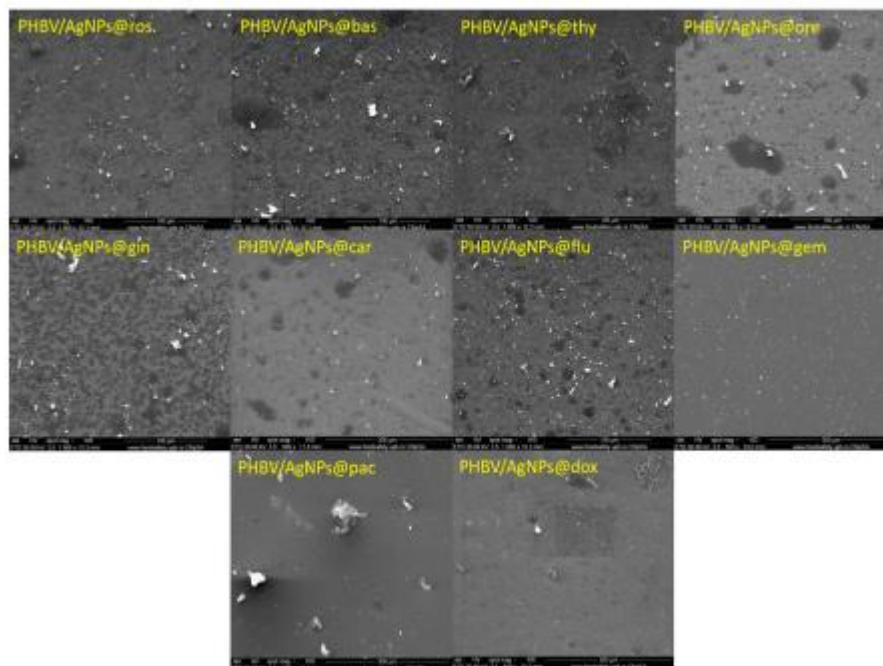


Figure 13: SEM images of the coatings (500–1000×) obtained at a laser fluence 400 mJ/cm².

To investigate the effect of PHBV/AgNP coatings loaded with natural compounds and anticancer drugs on the cell viability of both normal and tumor cells, the metabolic cell health was quantified by the MTT assay after 48 h and 5 days of cell-coating contact. The obtained results (Figure 14) showed that after 48 h of contact, all loaded samples impacted the cell survival of both normal and tumor cells, the cell viability being statistically significantly decreased by all coatings, independent of the drug load. Among anticancer drug-loaded coatings, PHBV/AgNPs@gem, PHBV/AgNPs@carb, and PHBV/AgNPs@dox showed the strongest potential to suppress the cell viability of the MC7 cells, while PHBV/AgNPs@pac and PHBV/AgNPs@flu exhibited a lower, but the still powerful, cytotoxic effect—reducing the cell viability by ~25% and ~33%, respectively, as compared with the untreated control. Concerning the normal cells, the anticancer-drug-loaded PHBV/AgNP coatings showed a similar cytotoxic potential, all samples triggering a statistically significant decrease of up to ~60% in the cell viability compared with the untreated control. In contrast, although there were samples loaded with natural compounds—which had effects similar to those loaded with chemotherapy compounds— PHBV/AgNPs@ros and PHBV/AgNPs@thy showed a more moderate impact on the normal cell survival, decreasing the cell viability only by ~30% compared to untreated control.

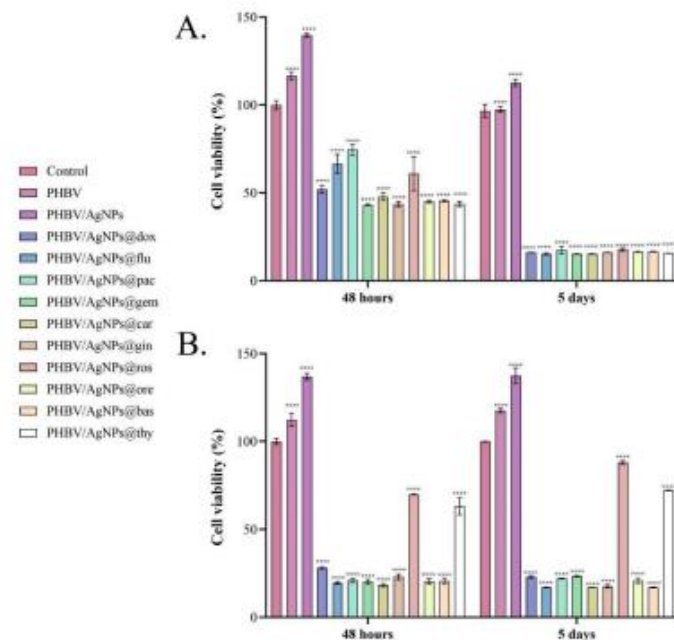


Figure 14: Graphical representation of cell viability of (A) MCF7 tumor cells and (B) VERO cells after 48 h and 5 days of contact with uncoated samples (control) and PHBV, PHBV containing cytostatic and PHBV containing essential oils

The cytotoxic profiles revealed by the LDH assay (Figure 15) confirmed the results obtained by the MTT assay. Comparing the LDH levels in all the drug-loaded PHBV/AgNPs samples, the lowest LDH levels were observed in the culture media harvested from the PHBV/AgNPs@flu samples.

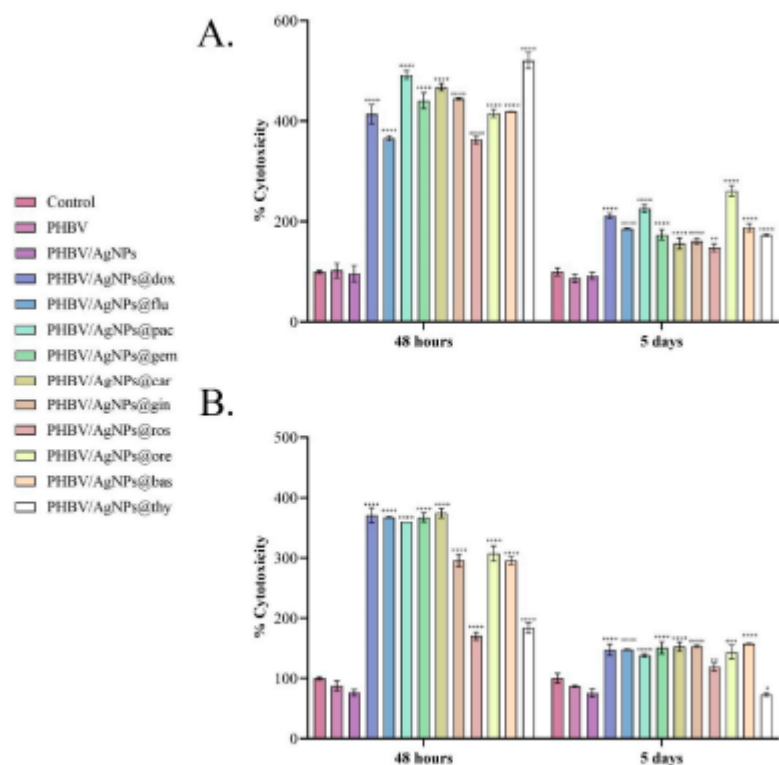


Figure 15. Graphical representation of uncoated samples (control) and PHBV, PHBV/AgNP, loaded with cytostatic and essential oils coating cytotoxicity as revealed by the LDH leakage levels quantified in culture media samples harvested from (A) MCF7 tumor cells and (B) VERO cells after 48h and 5 days with the experimental samples.

The obtained results showed that the natural-compound-loaded PHBV/AgNP coatings induced cytotoxic effects in both the tumor and the normal cells, similar to those induced by the anticancer-drug-loaded PHBV/AgNPs. Both MTT and LDH assays revealed that the cytotoxic effects were mediated by the drug payload of the PHBV/AgNP coatings, as pristine samples (PHBV and PHBV/AgNPs) did not negatively affect cell viability and cytotoxicity. Furthermore, the PHBV/AgNPs showed excellent biocompatibility with both the normal and the tumor cells, with a significant increase in cell viability being noticed when compared with the experimental reference. While the all-natural-compound-loaded PHBV/AgNP coatings significantly decreased the cell viability of the tumor cells, most of these samples showed a strong cytotoxic effect on the normal cells. However, rosemary and thyme, although they

triggered a decrease in the cell viability of the normal cells, were shown to be significantly less cytotoxic compared with the other samples while still presenting the same cytotoxic effect of traditional anticancer drugs on the tumor cell viability.

To evaluate the impact of drug loaded PHBV-PHBV/AgNPs on the normal and tumor cell morphologies, as well as the cell distribution on the material surfaces, the samples were analyzed by fluorescence microscopy after actin filaments and nuclei staining (Figure 16). The obtained results revealed that, in the absence of a drug load, all samples allowed the normal cells development of both the normal and the tumor cells. The addition of either anticancer drugs or natural compounds in the PHV-AgNPs structure triggered severe alterations of the cellular architecture on both the normal and the tumor cells, except for PHBV/AgNPs@ros and PHBV/AgNPs@thy, which altered with greater affinity the tumor cells morphology.

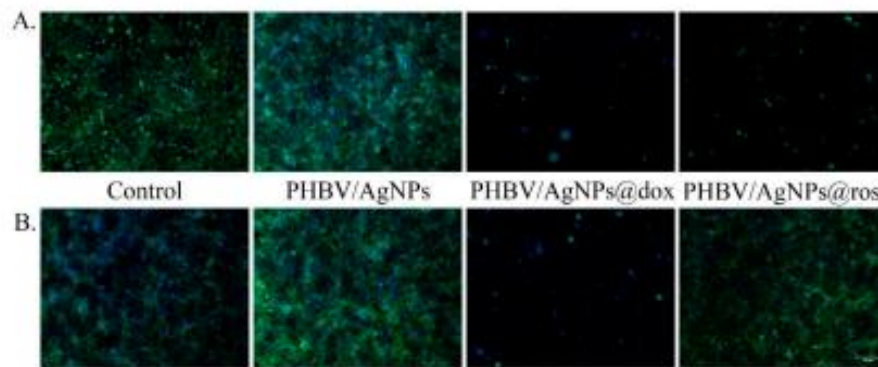


Figure 16 Fluorescence micrographs revealing (A) MCF7 cells and (B) VERO cells cytoskeleton after 5 days of contact with a reference sample, pristine PHBV/AgNPs, PHBV/AgNPs@dox, and PHBV/AgNPs@ros. Scale bare: 100 μm (green—actin filaments labeled with FITC-phalloidin; blue—cell nuclei stained with DAPI).

In order to analyze the antimicrobial effect of the tested coatings, several growth and viability tests in PBS were performed. Viability in PBS was assessed at two time points, i.e., 2 h and 24 h, in order to establish the bacteria-killing intrinsic potential of the nanocoated samples. Significant viability loss was observed in the presence of the coatings containing the Eos, especially PHBV/AgNPs@gin, PHBV/AgNPs@ros, PHBV/AgNPs@bas, and PHBV/AgNPs@thy. The viability of these coatings was significantly impaired at both tested time points (Figure 17). Regarding the biofilm development, no significant inhibition was observed in the case of the cytostatic-containing drug coatings in the tested conditions. However, a significant biofilm inhibition was observed in all coatings containing AgNPs and

EOs. Ginger and thyme EOs proved to have the highest anti-biofilm effects in all analyzed microbial strains, as revealed by Figure 18.

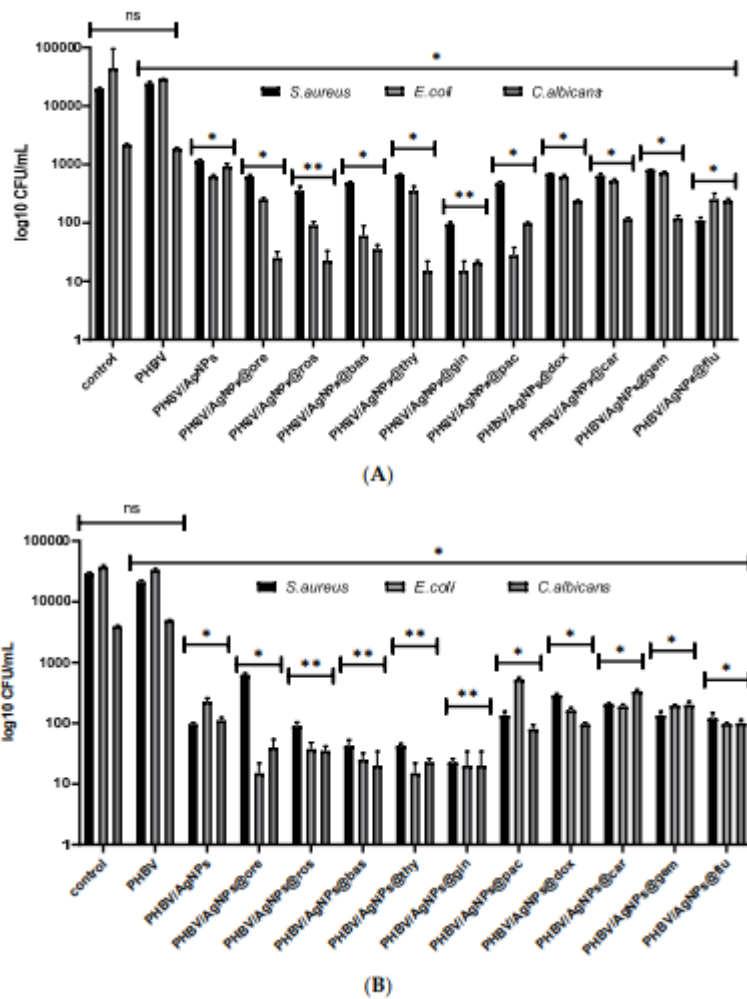


Figure 17. Graphical representation of log₁₀ CFU/mL values obtained for tested microbial strains, expressing viability of bacteria incubated as 0.5 McFarland suspensions in PBS on the obtained coatings for 2 h (A) and 24 h (B). * p < 0.05; ** p < 0.001 by comparing biofilm formation on PHVB control and each AgNPs coatings, ns—not significant.

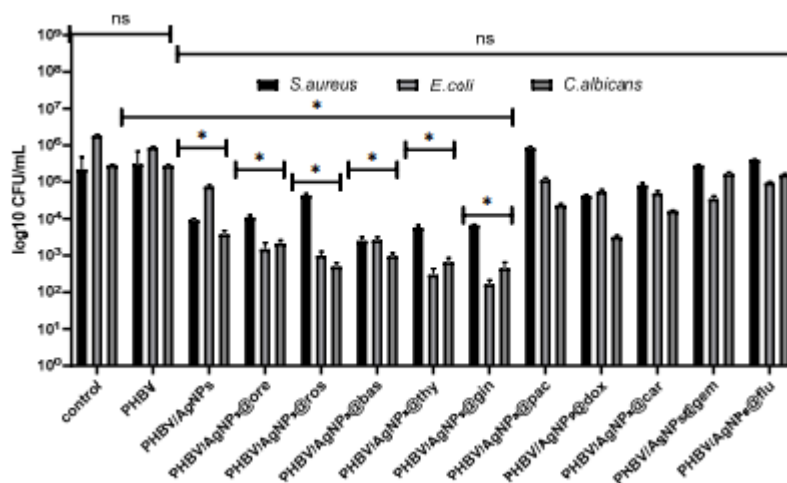


Figure 18. Graphic representation of log₁₀ CFU/mL values obtained for the tested microbial strains, expressing biofilm-embedded cells developed on control and AgNPs coatings for 24 h of incubation. * p < 0.05; by comparing biofilm formation of PHBV control and each AgNPs coatings.

General conclusions

Management of cancer patients gained a lot of interest lately, significant researches being made on new strategies development. Despite all advancement, clinical response of cancer patients to cancer treatment is limited, this leading to efficacy improvement by searching for alternatives. As a possible solution to these outcomes, natural compounds were studied as agents in cancer treatment and demonstrated to be effective to drug resistance improvement as well as possessing pharmacological effects.

Recent studies showed that Essential oils can be a promising therapeutic natural solution which contain a wide variety of chemical compounds, all of them having medical potential. The complex chemical structures found in essential oils can not be find in other natural agents, offering the advantages of being very available in nature, cost of production is low, and it also have the potential to be produced for a large-scale [49]. Of course, all of these advantages come with some weak points, essential oils being very volatile, poor solubility, low stability, and sometimes insufficient specific targeting.

These limitations can be overcome by nanomedicine, through nanotechnology approach, offering loading methods for essential oil to improve targeting of selected cells.

Smart nanocarriers loaded with customized pharmacokinetics which can be delivered directly to the targeted area are a solution to many hardships faced with conventional therapeutic approaches. Having a remarkable number of important characteristics, SPIONs present biocompatibility, the ability to target tumoral zones and causing death of cancer cells through hyperthermia.

PTX-loaded β -CD surface-modified SPIONs, both as nanopowders and thin films obtained by MAPLE technique seemed to have appropriate properties do be used as drug delivery systems for targeted tumors. The optimal beam fluence of laser was $400\text{mJ}/\text{cm}^2$, thin films having highest structural integrity. Magnetic nanocomposites present biocompatibility and cytotoxicity, sowed by MTT test performed on osteoblasts and osteosarcoma cells. Analyzing the obtained thin films after being loaded with PTX, it showed that they significantly increased the affinity for cancer cells.

Cytostatic drugs available at the moment represent a major problem for organism, attacking both normal cells and cancerous ones. Therefore, as a solution in facing this situation, in vitro studies were performed on MCF7 cell line and normal VERO cells of nanocoatings based on AgNPs loaded with cytostatic drugs (fludarabine, gemcitabine, carboplatin, doxorubicin and paclitaxel) and essential oils (rosemary, basil, ginger, thyme and oregano), obtained through MAPLE technique.

All obtained nanocoatings showed impressive cytotoxic activity against tumor cell lines, but the ones loaded with thyme and rosemary presented a remarkable cytotoxicity against cancer cells. As a confirmation of this result, AgNPs loaded with rosemary essential oil were tested on fluorescence microscopy, showing that in altered tumor cells with great affinity, while the effect was not so intense on normal cell line.

Obtained silver nanoparticles had dimensions ranged between 20 and 60nm, the ones functionalized with essential oils having bigger sizes.

The highest potential to eliminate MC7 cells' viability was present in coating containing gemcitabine, carboplatin and doxorubicine, while the ones containing paclitaxel and fludarabine showed a lower potential, cell viability being reduced by 33% and respectively 25%.

Tests for antibiofilm and antimicrobial activities were performed against *E. coli*, *S. aureus* and *Candida albicans*, cell viability being significantly decreased by all nanocoatings containing essential oils, the best antibiofilm activity being exhibited by AgNPs loaded with thyme and ginger.

As a general conclusion, it was demonstrated that natural compounds loaded nanocoatings presented similar cytotoxic activity as traditional cytostatic against cancer cells, the decrease of normal cell viability being much lower than the one caused by cytostatic drugs. This selective cytotoxicity is an important outcome which strongly recommends the new designed nanocoatings as another solution for cancer therapy, at least for breast cancer.

Bibliography

1. Ulu, G., Y. Kiraz, and Y. Baran. *Personalized biomedicine in cancer: from traditional therapy to sustainable healthcare*. 2020.
2. Rawal, S. and M.M.J.J.o.c.r. Patel, *Threatening cancer with nanoparticle aided combination oncotherapy*. 2019. **301**: p. 76-109.
3. Byrne, J.D., T. Betancourt, and L. Brannon-Peppas, *Active targeting schemes for nanoparticle systems in cancer therapeutics*. *Adv Drug Deliv Rev*, 2008. **60**(15): p. 1615-26.
4. Reddy Panyala, N., E. Peña-Méndez, and J. Havel, *Gold and nano-gold in medicine: Overview, toxicology and perspectives*. *Journal of Applied Biomedicine*, 2009. **7**.
5. Ulu, G.T., Y. Kiraz, and Y. Baran, *Chapter 22 - Personalized biomedicine in cancer: from traditional therapy to sustainable healthcare*, in *Biodiversity and Biomedicine*, M. Ozturk, D. Egamberdieva, and M. Pešić, Editors. 2020, Academic Press. p. 441-457.
6. Parveen, S., R. Misra, and S.K. Sahoo, *Nanoparticles: a boon to drug delivery, therapeutics, diagnostics and imaging*. *Nanomedicine*, 2012. **8**(2): p. 147-66.
7. Gabizon, A.A., R.T.M. de Rosales, and N.M. La-Beck, *Translational considerations in nanomedicine: The oncology perspective*. *Adv Drug Deliv Rev*, 2020. **158**: p. 140-157.
8. Raja, G., et al., *Microcellular Environmental Regulation of Silver Nanoparticles in Cancer Therapy: A Critical Review*. *Cancers (Basel)*, 2020. **12**(3).
9. Skóra, B., K.A. Szychowski, and J. Gmiński, *A concise review of metallic nanoparticles encapsulation methods and their potential use in anticancer therapy and medicine*. *European Journal of Pharmaceutics and Biopharmaceutics*, 2020. **154**: p. 153-165.
10. Abdal Dayem, A., et al., *The Role of Reactive Oxygen Species (ROS) in the Biological Activities of Metallic Nanoparticles*. *Int J Mol Sci*, 2017. **18**(1).
11. Bandeira, M., et al., *Green synthesis of zinc oxide nanoparticles: A review of the synthesis methodology and mechanism of formation*. *Sustainable Chemistry and Pharmacy*, 2020. **15**: p. 100223.
12. Vijayaraghavan, K. and T. Ashokkumar, *Plant-mediated biosynthesis of metallic nanoparticles: A review of literature, factors affecting synthesis, characterization techniques and applications*. *Journal of Environmental Chemical Engineering*, 2017. **5**(5): p. 4866-4883.
13. Abd El-Sadek, M.S., H.S. Wasly, and K.M. Batooh, *X-ray peak profile analysis and optical properties of CdS nanoparticles synthesized via the hydrothermal method*. *Applied Physics A*, 2019. **125**(4): p. 283.
14. Montero-Muñoz, M., et al., *Growth and formation mechanism of shape-selective preparation of ZnO structures: correlation of structural, vibrational and optical properties*. *Physical Chemistry Chemical Physics*, 2020. **22**(14): p. 7329-7339.
15. Shard, A.G., L. Wright, and C.J.B. Minelli, *Robust and accurate measurements of gold nanoparticle concentrations using UV-visible spectrophotometry*. 2018. **13**(6): p. 061002.
16. Keshavarz, M., et al., *Metal-oxide surface-enhanced Raman biosensor template towards point-of-care EGFR detection and cancer diagnostics*. 2020. **5**(2): p. 294-307.
17. Selmani, A., D. Kovačević, and K. Bohinc, *Nanoparticles: From synthesis to applications and beyond*. *Advances in Colloid and Interface Science*, 2022. **303**: p. 102640.
18. Mérai, L., et al., *Fast optical method for characterizing plasmonic nanoparticle adhesion on functionalized surfaces*. *Analytical and Bioanalytical Chemistry*, 2020. **412**(14): p. 3395-3404.
19. Lai, Y.H., et al., *Rapid screening of antibody–antigen binding using dynamic light scattering (DLS) and gold nanoparticles*. *Analytical Methods*, 2015. **7**(17): p. 7249-7255.
20. Garcia, P.R.A.F., et al., *An in situ SAXS investigation of the formation of silver nanoparticles and bimetallic silver–gold nanoparticles in controlled wet-chemical reduction synthesis*. *Nanoscale Advances*, 2020. **2**(1): p. 225-238.
21. Kim, A., et al., *Validation of Size Estimation of Nanoparticle Tracking Analysis on Polydisperse Macromolecule Assembly*. *Scientific Reports*, 2019. **9**(1): p. 2639.

22. Shivakumara, S., T.R. Penki, and N. Munichandraiah, *High specific surface area α -Fe₂O₃ nanostructures as high performance electrode material for supercapacitors*. Materials Letters, 2014. **131**: p. 100-103.
23. Conde, J., G. Doria, and P. Baptista, *Noble Metal Nanoparticles Applications in Cancer*. Journal of Drug Delivery, 2012. **2012**: p. 751075.
24. Efendic, F., et al., *Histological and biochemical apoptosis changes of female rats' ovary by Zinc oxide nanoparticles and potential protective effects of l-arginine: An experimental study*. Annals of Medicine and Surgery, 2022. **74**: p. 103290.
25. Lyu, Y., et al., *Synthesis of silver nanoparticles using oxidized amylose and combination with curcumin for enhanced antibacterial activity*. Carbohydrate Polymers, 2020. **230**: p. 115573.
26. Iqbal, S., et al., *Application of silver oxide nanoparticles for the treatment of cancer*. Journal of Molecular Structure, 2019. **1189**: p. 203-209.
27. Danişman-kalındemirtaş, f., et al., *Selective cytotoxicity of paclitaxel bonded silver nanoparticle on different cancer cells*. Journal of Drug Delivery Science and Technology, 2021. **61**: p. 102265.
28. Castañeda, A.M., et al., *Synergistic effects of natural compounds and conventional chemotherapeutic agents: recent insights for the development of cancer treatment strategies*. Heliyon, 2022. **8**(6): p. e09519.
29. Pairoj, S., et al., *Antiradical properties of chemo drug, carboplatin, in cooperation with ZnO nanoparticles under UV irradiation in putative model of cancer cells*. Biocybernetics and Biomedical Engineering, 2019. **39**(3): p. 893-901.
30. Sharma, A., A.K. Goyal, and G. Rath, *Recent advances in metal nanoparticles in cancer therapy*. Journal of Drug Targeting, 2018. **26**(8): p. 617-632.
31. Salehi, F., et al., *Stabilization of Zataria essential oil with pectin-based nanoemulsion for enhanced cytotoxicity in monolayer and spheroid drug-resistant breast cancer cell cultures and deciphering its binding mode with gDNA*. International Journal of Biological Macromolecules, 2020. **164**.
32. Sharma, M., et al., *Essential oils as anticancer agents: Potential role in malignancies, drug delivery mechanisms, and immune system enhancement*. Biomedicine & Pharmacotherapy, 2022. **146**: p. 112514.
33. Gudovan, D., et al., *Functionalized magnetic nanoparticles for biomedical applications*. Current Pharmaceutical Design, 2015. **21**(42): p. 6038-6054.
34. Dulińska-Litewka, J., et al., *Superparamagnetic Iron Oxide Nanoparticles-Current and Prospective Medical Applications*. Materials (Basel), 2019. **12**(4).
35. Puiu, R.A., et al., *Anti-Cancer Nanopowders and MAPLE-Fabricated Thin Films Based on SPIONs Surface Modified with Paclitaxel Loaded β -Cyclodextrin*. 2021. **13**(9): p. 1356.
36. Wang, Y.-X.J.J.Q.l.i.M. and Surgery, *Superparamagnetic iron oxide based MRI contrast agents: Current status of clinical application*. 2011, 2011. **1**(1): p. 35-40.
37. Rahmani, R., et al., *Plant-mediated synthesis of superparamagnetic iron oxide nanoparticles (SPIONs) using aloe vera and flaxseed extracts and evaluation of their cellular toxicities*. Ceramics International, 2020. **46**(3): p. 3051-3058.
38. Jafarizad, A., et al., *Gold Nanoparticles and Reduced Graphene Oxide-Gold Nanoparticle Composite Materials as Covalent Drug Delivery Systems for Breast Cancer Treatment*. 2017. **2**(23): p. 6663-6672.
39. Hyun, H., et al., *Engineered beta-cyclodextrin-based carrier for targeted doxorubicin delivery in breast cancer therapy in vivo*. Journal of Industrial and Engineering Chemistry, 2019. **70**: p. 145-151.
40. Jeon, H., et al., *Poly-paclitaxel/cyclodextrin-SPION nano-assembly for magnetically guided drug delivery system*. Journal of Controlled Release, 2016. **231**: p. 68-76.
41. Kong, T., et al., *Enhancement of Radiation Cytotoxicity in Breast-Cancer Cells by Localized Attachment of Gold Nanoparticles*. 2008. **4**(9): p. 1537-1543.

42. Musielak, M., I. Piotrowski, and W.M. Suchorska, *Superparamagnetic iron oxide nanoparticles (SPIONs) as a multifunctional tool in various cancer therapies*. Reports of Practical Oncology & Radiotherapy, 2019. **24**(4): p. 307-314.
43. Miller, K.D., et al., *Cancer statistics for adolescents and young adults, 2020*. 2020. **70**(6): p. 443-459.
44. Chi, Y.-N., et al., *Development of protective agents against ovarian injury caused by chemotherapeutic drugs*. Biomedicine & Pharmacotherapy, 2022. **155**: p. 113731.
45. Fares, J.E., et al., *Metronomic chemotherapy for patients with metastatic breast cancer: Review of effectiveness and potential use during pandemics*. Cancer Treatment Reviews, 2020. **89**: p. 102066.
46. Papavlu, A.P., et al., *Matrix-assisted pulsed laser evaporation of organic thin films: Applications in biology and chemical sensors*. 2017: p. 171-189.
47. Bonciu, A., et al., *Interfaces obtained by MAPLE for chemical and biosensors applications*. Sensors and Actuators Reports, 2021. **3**: p. 100040.
48. Zhai, Y., et al., *Synthesis of magnetite nanoparticle aqueous dispersions in an ionic liquid containing acrylic acid anion*. Colloids and Surfaces A: Physicochemical and Engineering Aspects, 2009. **332**(2): p. 98-102.
49. AbouAitah, K. and W. Lojkowski, *Nanomedicine as an Emerging Technology to Foster Application of Essential Oils to Fight Cancer*. Pharmaceuticals (Basel), 2022. **15**(7).